

# A CFD ANALYSIS OF THE INFLUENCE OF PLENUM CONFIGURATIONS ON GAS DISTRIBUTION IN A FLUIDIZED BED

J. M. SORIA<sup>†</sup>, T. M. AUSINA<sup>‡</sup>, and G. D. MAZZA<sup>†</sup>

<sup>†</sup> *Institute for Research and Development in Process Engineering, Biotechnology and Alternative Energies, (PROBIEN, CONICET - UNCo), 1400 Buenos Aires St., 8300, Neuquén, Argentina.*

<sup>‡</sup> *Chemical Department, Engineering Faculty, National University of Comahue (UNCo), 1400 Buenos Aires St., 8300, Neuquén, Argentina.*

*jose.soria@probien.gob.ar, german.mazza@probien.gob.ar*

**Abstract** — Fluidized beds are widely used in many industries. The fluidization quality of these units is strongly related to the characteristics of the plenum and distributor (grid). In this work, the effect of different plenum geometries, and gas entrance sizes and locations on the velocity profile above the distributor was analyzed by Computational Fluid Dynamics (CFD). The results showed that flow uniformity above the distributor improved with an increase in the gas inlet diameter and the plenum height. Channeling was observed for the bottom central inlet. Additionally, simulations for plenum heights predicted by one of the frequently used correlations (Litz correlation) were also carried out and showed, especially for a bottom central gas inlet, a poor quality flow distribution. This behavior indicated that Litz correlation tends to underestimate the plenum height for obtaining a uniform flow downstream the distributor.

**Keywords**— CFD, Plenum chamber, Distributor, Flow uniformity, Gas-solid fluidized bed.

## I. INTRODUCTION

Fluidized beds are widely used in industrial operations due to their numerous advantages, which include excellent mixing capabilities and high mass and heat transfer rates (Gupta and Sathyamurthy, 1999). However, if the quality of fluidization is poor, heat and mass transfer rates are reduced significantly and the overall performance of fluid bed decays. In this sense, the design of the distribution system (plenum and distributor) is a primary factor so as to achieve an even distribution of the fluidizing agent (gas) and improve the fluidization quality. The knowledge of the gas flow distribution over the whole domain of a fluidized bed is essential for the comprehension of the hydrodynamics of the unit (Depypere *et al.*, 2004).

Pressure drop across the distributor has traditionally been the main criteria when designing distributors (Geldar and Baeyens, 1985). In fact, distributors with high pressure drop tend to even the gas distribution in spite of more power consumption of compressors and fans. Thus, in order to minimize the cost of the gas supply system, low pressure drop distributors that guarantee a good fluidization are highly desirable. Nonetheless, low pressure distributors may cause a poor fluidization with gas channeling and inefficient mixing of particles. In the latter

context (low grid-pressure-drop-to-bed pressure-drop ratio), the plenum chamber or *windbox*, located immediately below the grid, becomes crucial for achieving a uniform gas velocity profile above the grid and the bed operating satisfactorily.

The most common criteria for the design of the plenum and distributor are empirical:

- the pressure drop across the distributor ( $\Delta P_d$ ) is related to the pressure drop across the bed,  $\Delta P_b$ , (Kunii and Levenspiel, 1991), as follows:

$$\Delta P_d = (0.2 - 0.4)\Delta P_b \quad (1)$$

- Litz (1972) proposed to estimate the plenum height ( $H_p$ ) based on the plenum diameter ( $D_p$ ) and gas inlet diameter ( $D_e$ ). Thus, when the gas entered by a side of a plenum as:

$$H_p = 0.2D_p + 0.5D_e, \quad \text{if } D_e > D_p/100 \quad (2a)$$

$$H_p = 18D_e, \quad \text{if } D_e < D_p/100 \quad (2b)$$

and for the bottom entry:

$$H_p = 3(D_p - D_e), \quad \text{if } D_e > D_p/36 \quad (2c)$$

$$H_p = 100D_e, \quad \text{if } D_e < D_p/36 \quad (2d)$$

These rules do not allow defining the crucial characteristics of the gas flow. Moreover, it is almost impossible to perform an experimental study of the gas flow pattern because of the diversity of configurations of the windbox -height to diameter ratio, nozzle location and diameter- and grids characteristics (Dhotre and Joshi, 2003).

The complex flow dynamics and the development of robust numerical tools have promoted the Computational Fluid Dynamics (CFD) as an efficient mean for the comprehensive analysis of the behavior of fluidized beds (Mohammadkhah and Mostoufi, 2009). However, most of the works that simulate the fluid bed hydrodynamics by CFD, consider a uniform gas velocity entrance, while neglecting the effect of the plenum or the distributor (Taghipour *et al.*, 2005). On the other hand, several studies have reported the relevance of taking into account the plenum geometry and the distributor when simulating the fluid bed unit, since it may present a significant impact on the bed performance. Thus, the assumption of a uniform velocity profile above the distributor might not be adequate (Depypere *et al.*, 2004).

In this frame, two objectives are set in this work. The first aim is to use CFD in order to study the influence of several plenum configurations on the flow pattern in the plenum, as well as on the gas velocity profile above the distributor. The gas uniformity for plenum heights according to Litz correlations is additionally analyzed.

## II. CFD MODELLING APPROACH

### A. Computational domain geometry and meshing

The fluid dynamic behavior in the plenum was predicted by means of a CFD model that involves complex 3D turbulent flow. The model geometry comprises a cylindrical plenum of 15 cm in diameter, while different heights were analyzed ( $H_p = 4.1, 5.6, 15, 20, 29.76$  and  $37.38$  cm). Two nozzle diameters were also studied (2.54 and 5.08 cm). The distributor was 1 cm thick and two inlet positions were studied: bottom central and side bottom. In order to avoid possible numerical drawbacks, mainly gas backflow, the computational domain was extended by including a 10-cm height zone above the grid.

The mesh was generated with tetrahedral elements. Special care was taken in refining the mesh in the zones where significant gradients are expected to occur: (1) before and after the distributor by reducing the elements sizes, and (2) near the walls by performing inflation. However, larger elements were considered for the distributor zone in order to satisfy the porous media condition applied in that region. Once the tetrahedral mesh is obtained, a re-mesh procedure was applied in order to obtain polyhedral control volumes. This technique allowed reducing considerably the elements number (around 70%), without reducing the mesh quality, while improving convergence in lesser number of iterations. The quality of the mesh was checked based on parameters such as skewness, aspect ratio and orthogonal quality. Figure 1 shows a view (y-z plane) of one adopted geometry along with the boundary conditions.

Finally, mesh characteristics were validated when the solution was independent of the grid. As a result, the computational domain varied between 1028807 and 3443325 polyhedral elements, depending on the plenum configuration.

### B. Governing Equations

The mass conservation (Eq. 3) and the momentum conservation (Eq. 4) equations were solved numerically.

$$\nabla(\rho\vec{U}) = 0 \quad (3)$$

$$\nabla(\rho\vec{U}\vec{U}) = -\nabla P + \nabla\vec{\tau} + \rho\vec{g} + S_i \quad (4)$$

where  $\rho$  stands for the fluid density,  $\vec{U}$  is the velocity vector,  $P$  the static pressure and  $S_i$  represents a sink term which is considered for modelling the distributor as a porous media. The sink term is composed by two contributions: one related to viscous loss and the second one for inertial losses (Eq. 5).

$$S_i = -(\mu/\alpha)U_i + C_2(1/2)\rho|U|U_i \quad (5)$$

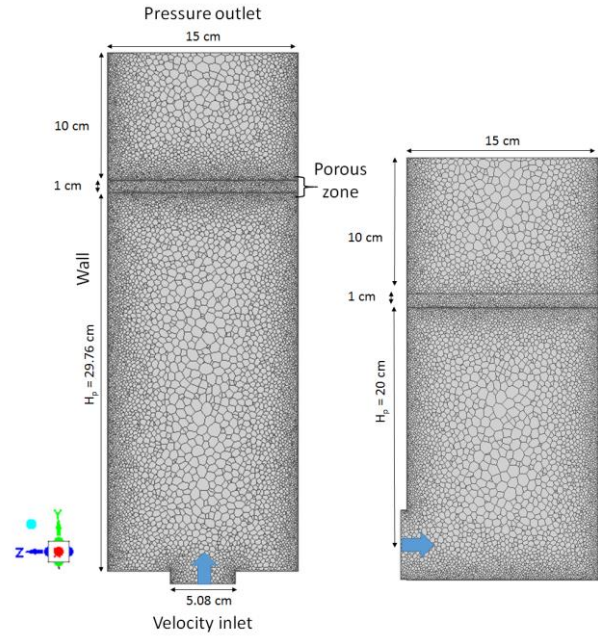


Figure 1. Polyhedral mesh and boundary conditions of the computational domain (case: bottom central inlet).

Turbulence equations were solved with  $k-\varepsilon$  *realizable* model. The governing equations are given by:

$$\nabla(\rho U k) = \nabla[(\mu + (\mu_t/\sigma_k))\nabla k] + G_k - \rho\varepsilon \quad (6)$$

$$\nabla(\rho U \varepsilon) = \nabla[(\mu + (\mu_t/\sigma_\varepsilon))\nabla \varepsilon] - C_{2\varepsilon}\rho(\varepsilon^2/k + \sqrt{\varepsilon\nu}) \quad (7)$$

The turbulent viscosity ( $\mu_t$ ) is related to  $k$  and  $\varepsilon$  as shown in Eq. (8):

$$\mu_t = C_\mu\rho(k^2/\varepsilon) \quad (8)$$

The default  $k-\varepsilon$  *realizable* model parameters were selected:  $C_{1\varepsilon} = 1.44$ ,  $C_{2\varepsilon} = 1.9$ ,  $\sigma_k = 1.0$ ,  $\sigma_\varepsilon = 1.2$ . Additionally, as turbulent flows are affected by the presence of walls, *Enhanced Wall Treatment* method was used, with  $y^+$  values lower than five (ANSYS, 2016).

### C. Material properties and boundary conditions

The distributor was considered as a sintered plate located above the plenum chamber. The distributor was designed following Kunii and Levenspiel (1991) recommendations (eq. 1), for a case of Geldart B particles (500  $\mu\text{m}$  sand,  $\rho_s = 2650 \text{ kg}\cdot\text{m}^{-3}$ ,  $U_{mf} = 0.2195 \text{ m}\cdot\text{s}^{-1}$ ) and an initial ratio of bed height to bed diameter equal to 1. The distributor was modelled as a porous media with a pressure drop of 530 Pa ( $\Delta P_d = 0.3 \Delta P_b$ ). Both permeability ( $\alpha$ ) and inertial resistance ( $C_2$ ) were taken from literature (Depypere *et al.*, 2004) as  $2.73 \times 10^{-11} \text{ m}^2$  y  $34500 \text{ m}^{-1}$ . Then, the distributor thickness ( $\Delta m = 0.01 \text{ m}$ ) was calculated from equation:

$$\Delta P_b = -(\mu U/\alpha + 0.5C_2\rho U^2)\Delta m \quad (9)$$

The fluidizing agent considered is air, where physical properties were assumed to remain constant ( $\rho = 1.225 \text{ kg}\cdot\text{m}^{-3}$ ,  $\mu = 1.7894 \times 10^{-5} \text{ kg}\cdot\text{m}^{-1}\cdot\text{s}^{-1}$ ), due to the low pressure drop through the computation domain to the operating pressure.

Table 1. Main solving parameters.

Variable	First Step		Second Step	
	URF	DS	URF	DS
Pressure	0.3	2 <sup>nd</sup> order	0.3	2 <sup>nd</sup> order
Momentum	0.7	1 <sup>st</sup> order	0.4	3 <sup>rd</sup> order
TKE	0.8	1 <sup>st</sup> order	0.1	3 <sup>rd</sup> order
TDR	0.8	1 <sup>st</sup> order	0.1	3 <sup>rd</sup> order
TV	1	1 <sup>st</sup> order	0.1	3 <sup>rd</sup> order

The gas velocity at the inlet was estimated with Bernoulli equation, by considering a bubbling regime ( $U = 3U_{mf}$ ) in the fluidized bed. Then, the gas velocity was 5.8 and 23.2 m.s<sup>-1</sup> for inlet diameters of 5.08 and 2.54 cm, respectively. The grid was considered as a porous media. Pressure outlet was fixed at the top of the geometry. The pressure value was set constant and equal to the atmospheric pressure. Finally, walls were specified as stationary walls with non-slip condition.

### D. Numerical solution

The simulations were performed three-dimensionally using FLUENT 17.2 CFD code (ANSYS Inc.), adopting a scheme of single precision steady-state with segregated implicit solver (Ranade, 2002).

The pressure-based method was applied to solve the Navier–Stokes equation. The pressure velocity coupling was performed through the SIMPLEC algorithm. Numerically, the simulations were carried out into two steps. The first one was performed under first order discretization schemes along with the default values. Once the solution converged, the second step began. In this stage, MUSCL third order discretization schemes (DS) for all variables was adopted and under-relaxation factors (URF) for turbulent kinetic energy (TKE), turbulent dissipation rate (TDR) and turbulent viscosity (TV) were set at 0.1 to minimize residual oscillation. Table 1 summarizes the main numerical solving parameters used in the simulations. An iterative numerical procedure was adopted to solve the governing equations, with a stricter convergence criteria. To perform the numerical technique, convergence was evaluated in two ways: (1) by the drop in the residuals  $\cdot 10^{-6}$  and (2) verifying the pressure drop remained constant through iterations.

## III. RESULTS AND DISCUSSION

In order to quantify the quality of distribution, the coefficient of variation (resulted from a statistical analysis) is used. It can be defined as the ratio between the standard deviation  $\sigma$  (m.s<sup>-1</sup>) of the velocity distribution above the porous plate and the mean gas velocity  $\bar{U}$ (m.s<sup>-1</sup>):

$$C_v = \sigma / \bar{U} \quad (9)$$

Results regarding the influence of the main parameters are presented in the following subsections.

### A. Influence of plenum height

Tables 2 and 3 present the results of air uniformity above the distributor for the gas entering at the bottom side and bottom central, respectively.

Table 2. Coefficient of variation for side bottom gas inlet (\* values for  $H_p$  according to Litz correlation).

$H_p$ [cm]	$D_e = 5.08$ cm	$D_e = 2.54$ cm
	$C_v = \sigma / \bar{U}$	$C_v = \sigma / \bar{U}$
4.1	-	0.0822*
5.6	0.0109*	-
15	0.0079	0.0292
20	0.0065	0.0072

Table 3. Coefficient of variation for bottom central gas inlet (\* values for  $H_p$  according to Litz correlation).

$H_p$ [cm]	$D_e = 5.08$ cm	$D_e = 2.54$ cm
	$C_v = \sigma / \bar{U}$	$C_v = \sigma / \bar{U}$
20	0.0102	0.0468
29.76	0.0089*	0.0366
37.38	0.0086	0.0258*

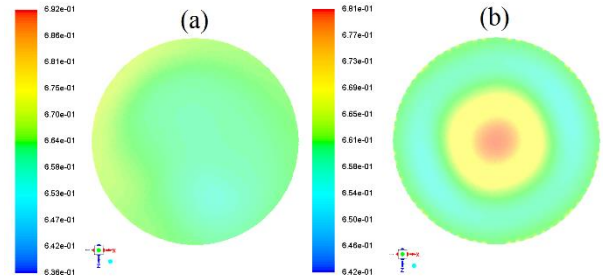


Figure 2. Contour plot of gas velocity magnitude above the distributor for  $D_e = 5.08$  cm and  $H_p = 20$  cm: (a) side entry, and (b) bottom entry.

The worst gas distribution was obtained for the lowest plenums (Litz correlation). In these cases, the gas path is not long enough to develop a uniform flow. For the side gas entry, the uneven distribution was reduced significantly when the plenum height increased from 5.6 to 20 cm. Then, a further increase in the plenum height seemed not to produce a significant improvement on flow uniformity.

It can be appreciated that as the  $H_p/D_p$  ratio increased, the flow became more uniform across the porous plate. In fact, an increase in the plenum height provides the air a longer path that favors the turbulence free flow (Jangam *et al.*, 2009). A similar trend was observed for the 2.54 cm nozzle, although the gas flow maldistribution is higher than that obtained for the 5.08 cm inlet.

### B. Influence of the position of gas entrance

The location of the gas inlet had a considerable effect on the flow pattern in the plenum as well as on the gas uniformity above the distributor. Figures 2a and 2b present the gas velocity profile above the distributor for a plenum height of 20 cm and  $D_e = 5.08$  cm. It can be seen that the side nozzle (Fig. 2a) produced a more uniform flow downstream the plate. In fact, for the bottom central nozzle, some central channeling was observed while for the case of lateral entry a more uniform distribution was obtained.

The flow pattern in the plenum is also affected by the location of the gas inlet. Figure 3 presents the path lines regarding the simulations for a plenum height of 20 cm

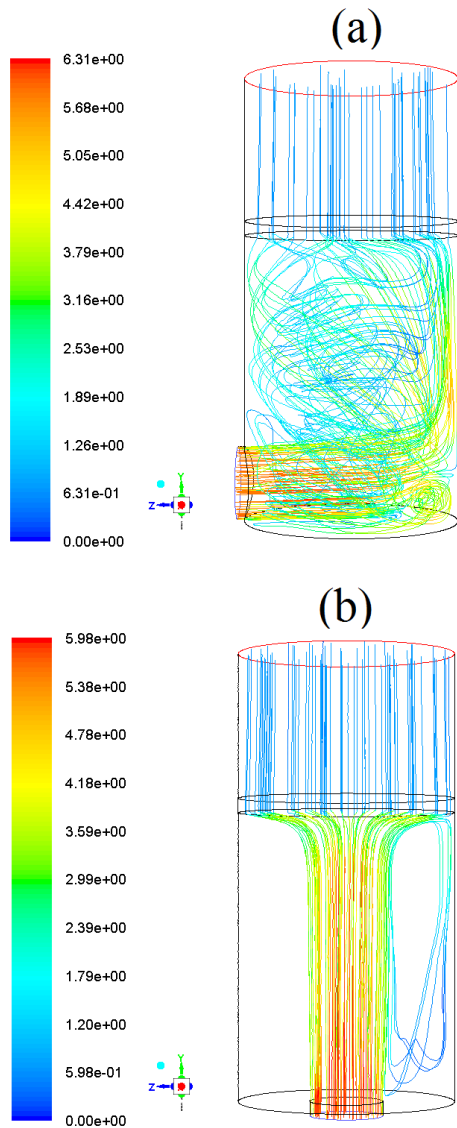


Figure 3. Path lines for different inlet locations: (a) bottom side, and (b) bottom central. Case:  $D_e = 5.08$  cm,  $H_p = 20$  cm.

and a 5.08 cm inlet. From Fig.3a, it can be seen that when the gas enters the plenum from a side, it hits the opposite wall and deviates mainly towards the distributor. A fraction of the gas adjacent to the wall passes through the distributor directly while the other fraction recirculates in the plenum and finally leaves the distributor. On the other hand, for a bottom central entry case (Fig. 3b), most of the gas is distributed directly, with limited recirculation. However, for the latter case, the gas velocity at the center of the distributor is slightly higher than that close to the walls.

**C. Influence of nozzle size**

The effect of gas inlet diameter on flow distribution was also analyzed. Figure 4 presents the velocity profiles for different configurations. It was observed that the 2.54 cm inlet (Fig. 4a) produced a worse gas distribution than the 5.08 entry (b). The kinetic head ( $U_{inlet}^2/2$ ) in the smaller inlet is significantly higher than that for the larger inlet.

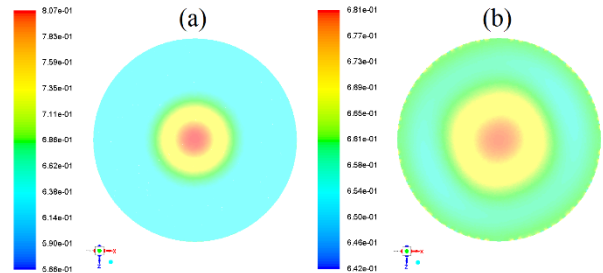


Figure 4. Velocity profile above the distributor: (a)  $D_e = 2.54$  cm, and (b)  $D_e = 5.08$  cm ( $H_p = 20$  cm, bottom central inlet).

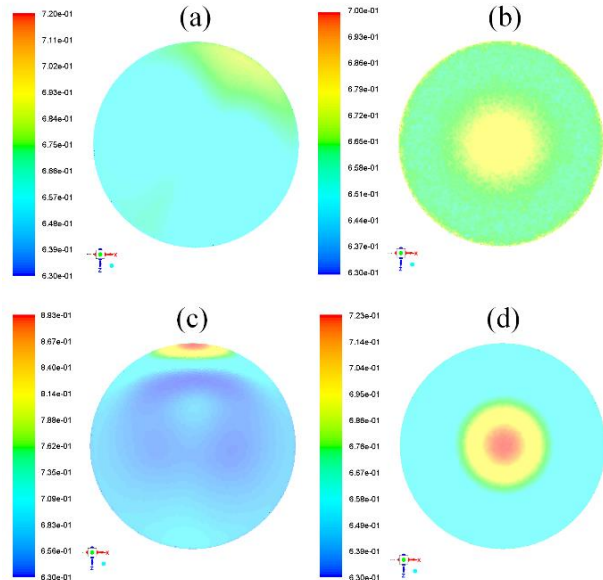


Figure 5. Contour plot of gas velocity magnitude above the distributor for plenum heights according to Litz correlation, (a)  $D_e = 5.08$  cm,  $H_p = 5.6$  cm and side entry, (b)  $D_e = 5.08$  cm,  $H_p = 29.76$  cm and bottom entry, (c)  $D_e = 2.54$  cm,  $H_p = 4.1$  cm and side entry, and (d)  $D_e = 2.54$  cm,  $H_p = 37.38$  cm and bottom entry.

Consequently, the gas arrived at the grid at a higher velocity producing a non-even gas distribution, with a higher-velocity central region. Thus, the larger the inlet diameter, the lower the kinetic head and the better the gas uniformity at the top of the distributor plate.

Additionally, it was observed that the maldistribution was reduced by increasing the plenum height, but it was not totally eliminated. Therefore, it can be inferred that the influence of the inlet size seems to be play a key role in gas uniformity, when compared with the effect of the plenum height.

**D. Comparison with Litz correlation (Litz, 1972)**

CFD results showed an uneven gas velocity distribution above the distributor for all plenum heights calculated from Litz correlation, given by high values of  $C_v$  (Tables 2 and 3). Moreover, CFD simulations contour plots (Fig. 5) showed that, for a side entry (Fig. 5a and 5c), the higher velocity values occurred at the opposite side of the inlet. For a bottom central nozzle, the higher gas velocities were predicted at the center of the distributor (Fig. 5b and 5d).

Table 4. Coefficient of variation for different pressure drop across the distributor. Case: 5.08 cm side inlet.

$H_p$ [cm]	$C_v = \sigma/\bar{U}$
20 ( $\Delta P_d = 0.3 \Delta P_b$ )	0.0065
20 ( $\Delta P_d = 0.2 \Delta P_b$ )	0.0088
20 ( $\Delta P_d = 0.15 \Delta P_b$ )	0.0106

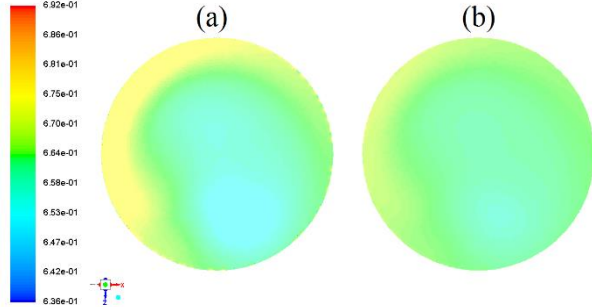


Figure 6. Contour plots above the distributor for different plenum pressure drop: (a)  $\Delta P_d = 0.15 \Delta P_b$ , and (b)  $\Delta P_d = 0.3 \Delta P_b$ . Case: 5.08 cm side inlet,  $H_p = 20$  cm.

**E. Influence of distributor pressure drop**

In order to analyze the influence of pressure drop across the distributor, different values of  $\alpha$  and  $C_2$  were considered, so as to obtain a ratio between the pressure drop in the distributor and the bed of 0.15, 0.2 and 0.3 (Table 4), while maintaining the grid thickness.

Results indicated that, for the case of a 5.08 cm side entry, the lower pressure drop distributor presented a more heterogeneous velocity profile, given by a larger standard deviation. An increase in the distributor pressure drop increased the flow resistance and improved the flow uniformity (Fig. 6), which is in agreement with observations reported elsewhere (Dhotre and Joshi, 2003; Janagam *et al.*, 2009).

**F. Influence of the side entrance height**

The effect of the side entrance height on the flow distribution was also analyzed. To this end, a CFD simulation of a plenum with a height of 30 cm (while fixing the position of the inlet at 20 cm) was carried out. Fig. 7 presents the path lines for this plenum.

Comparing Fig. 3.a with Fig. 7, it can be seen that the position of the gas entrance modified the flow pattern inside the plenum. Therefore, the velocity profile above the distributor was also influenced (Fig. 8), which resulted in a  $C_v$  value equal to 0.0077, slightly higher than the  $C_v$  obtained for  $H_p = 20$  cm. This increase in the flow non-uniformity can be explained on the basis of the interaction between the considerable amount of gas recirculation below the gas entrance and the main stream that enters the vessel.

**IV. CONCLUSIONS**

A CFD analysis of different plenum configurations on gas flow uniformity above the grid of a fluidized bed was carried out in this work. It was observed that different design parameters present a significant influence on the velocity profile downstream the distributor. The main conclusions can be drawn as follows:

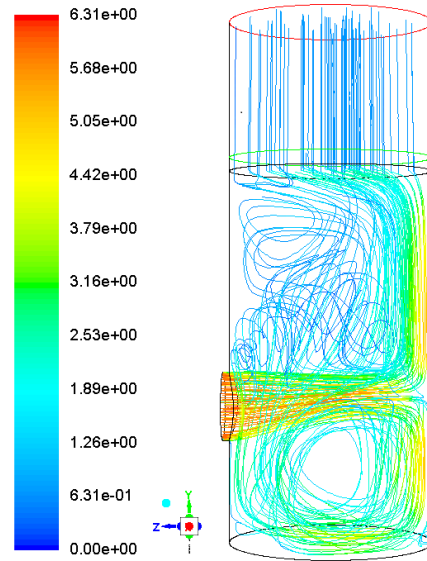


Figure 7. Path lines for side inlet. Case  $D_e = 5.08$  cm,  $H_e = 20$  cm and  $H_p = 30$  cm.

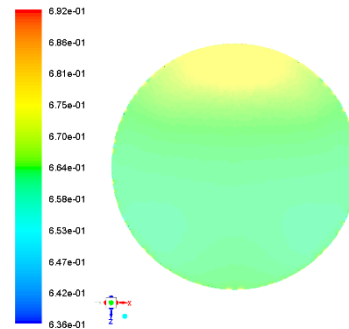


Figure 8. Contour plot of gas velocity magnitude above the distributor for  $D_e = 5.08$  cm,  $H_e = 20$  cm and  $H_p = 30$  cm.

- A more uniform gas velocity above the distributor was noted when increasing the plenum height.
- The gas inlet diameter stands as a key factor on the flow pattern. An increase in the nozzle size improved significantly the velocity profile uniformity above the grid.
- The gas-inlet location influenced the gas trajectory. A horizontal inlet increased the gas path, provoking a more even gas distribution.
- As expected, the higher the pressure drop in the distributor the better the flow uniformity.
- Litz correlation under predicted the plenum height for all the conditions analyzed in this work, giving a non-uniform gas velocity profile. Moreover, the worst case took place for the smallest inlet size.

**ACKNOWLEDGMENTS**

The authors wish to thank the support of the following Argentine institutions: ANPCyT – MINCyT (PICT No. 2014-2078), CONICET and SECITI – San Juan (PIO – CONICET – SECITI No. 15020150100042CO). José Soria and Germán Mazza are research members of CONICET, Argentina.

## NOMENCLATURE

$C_2$	inertial resistance ( $m^{-1}$ )
$C_v$	coefficient of variation (–)
$D_e$	diameter of the entrance (m)
$D_p$	diameter of the plenum (m)
$\vec{g}$	gravity vector ( $m.s^{-2}$ )
$H_e$	distance between the nozzle centerline and the distributor plate, (m)
$H_p$	plenum height, (m)
$k$	kinetic turbulent energy ( $m^2.s^{-2}$ )
$P$	pressure (Pa)
$U$	fluid velocity ( $m.s^{-1}$ )
$U_{mf}$	minimum fluidization velocity ( $m.s^{-1}$ )
$\alpha$	viscous resistance ( $m^{-2}$ )
$\Delta P_b$	bed pressure drop (Pa)
$\Delta P_d$	distributor pressure drop (Pa)
$\Delta m$	distributor thickness (m)
$\varepsilon$	turbulent dissipation rate ( $m^2.s^{-3}$ )
$\mu$	fluid dynamic viscosity (Pa.s)
$\mu_t$	turbulent viscosity (Pa.s)
$\rho$	fluid density ( $kg.m^{-3}$ )
$\rho_s$	solid density ( $kg.m^{-3}$ )
$\sigma$	standard deviation ( $m.s^{-1}$ )
$\sigma_\varepsilon$	turbulent Prandtl number in $\varepsilon$ equation
$\sigma_k$	turbulent Prandtl number in $k$ equation
$\bar{\tau}$	stress tensor (Pa)

## REFERENCES

- ANSYS (2016) *Theory guide 17.2*. ANSYS Inc. USA.
- Depypere, F., Pieters, J.G. and Dewettinck, K. (2004). “CFD analysis of air distribution in fluidised bed equipment,” *Powder technology*, **145**, 176-189.

- Dhotre, M.T. and Joshi, J.B. (2003). “CFD simulation of gas chamber for gas distributor design,” *The Canadian Journal of Chemical Engineering*, **81**, 677-683.
- Geldart, D. and Baeyens, J. (1985). “The design of distributors for gas-fluidized beds,” *Powder Technology*, **42**, 67–78.
- Gupta, C.K. and Sathyamurthy, D. (1999). *Fluid Bed Technology in Material Processing*, CRC Press.
- Jangam, S.V., Mujumdar, A.S. and Thorat, B.N. (2009). “Design of an efficient gas distribution system for a fluidized bed dryer,” *Drying Technology*, **27**, 1217-1228.
- Kunii, D. and Levenspiel, O. (1991). *Fluidization engineering*, Elsevier.
- Litz, W.J. (1972). “Design of Gas Distributors,” *Chemical Engineering*, **13**, 162-166.
- Mohammadkhan, A. and Mostoufi, N. (2009). “Effect of geometry of the plenum chamber on gas distribution in a fluidized bed,” *Industrial & Engineering Chemistry Research*, **48**, 7624-7630.
- Ranade, V.V. (2001). *Computational flow modeling for chemical reactor engineering*, Elsevier.
- Taghipour, F., Ellis, N. and Wong, C. (2005). “Experimental and computational study of gas–solid fluidized bed hydrodynamics,” *Chemical Engineering Science*, **60**, 6857-6867.

Received October 21, 2019

Sent to Subject Editor October 22, 2019

Accepted December 26, 2019

Recommended by Guest Editor: Carlos Apesteguia